Inorganic Chemistry

Article

Reaction Mechanism of the Dinuclear Zinc Enzyme N-Acyl-L-homoserine Lactone Hydrolase: A Quantum Chemical Study

Rong-Zhen Liao,[†,‡] Jian-Guo Yu,[‡] and Fahmi Himo*,[†]

Department of Theoretical Chemistry, School of Biotechnology, Royal Institute of Technology, SE-10691 Stockholm, Sweden, and College of Chemistry, Beijing Normal University, Beijing, 100875, People's Republic of China

N-acyl-L-homoserine lactone hydrolase (AHL lactonase) is a dinuclear zinc enzyme responsible for the hydrolytic ring opening of AHLs, disrupting quorum sensing in bacteria. The reaction mechanism is investigated using hybrid density functional theory. A model of the active site is designed on the basis of the X-ray crystal structure, and stationary points along the reaction pathway are optimized and analyzed. Two possible mechanisms based on two different substrate orientations are considered. The calculations give support to a reaction mechanism that involves two major chemical steps: nucleophilic attack on the substrate carbonyl carbon by the bridging hydroxide and ring opening by direct ester C−O bond cleavage. The roles of the two zinc ions are analyzed. Zn1 is demonstrated to stabilize the charge of the tetrahedral intermediate, thereby facilitating the nucleophilic attack, while Zn2 stabilizes the charge of the alkoxide resulting from the ring opening, thereby lowering the barrier for the C−O bond cleavage.

I. Introduction

In a phenomenon termed quorum sensing, bacteria communicate with one another through extracellular signaling molecules called autoinducers to monitor their own population density and to modulate gene expression.[1,2] In Gram-negative bacteria, quorum sensing is mostly carried out by N-acyl-L-homoserine lactones (AHLs). AHL autoinducers all share the homoserine moiety but differ in the length of their acyl chain and in the presence or absence of double bonds or functional groups.[2] These structural variations are responsible for the signaling specificity of AHLs.[3]

There are two different types of enzymes that can impede AHL activity. One is N-acyl-L-homoserine lactone hydrolase (AHL lactonase), which catalyzes the hydrolytic ring opening of AHLs (Scheme 1).[4] The other is N-acyl-L-homoserine lactone acylase, found in several different types of bacteria, including *Ralstonia* strain XJ12B, pseudomonads, and a

Scheme 1. Reaction Catalyzed by AHL Lactonase
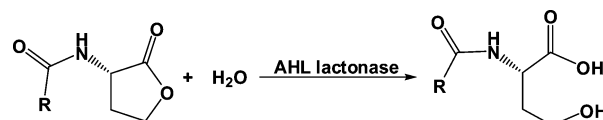
Streptomyces species, and cleaves the N-acyl bond of AHLs.[5] Given their importance in pathogenicity, quorum-sensing pathways have been suggested as potential targets for the development of new therapeutics against bacterial infections.[6]

AHL lactonase from *Bacillus thuringiensis* is a monomeric enzyme containing in the active site two Zn^{2+} ions that are

---

* To whom correspondence should be addressed. E-mail: himo@theochem.kth.se.
† Royal Institute of Technology.
‡ Beijing Normal University.
(1) (a) Fuqua, C.; Winans, S. C.; Greenberg, E. P. *Annu. Rev. Microbiol.* **1996**, *50*, 727–751. (b) Robson, N. D.; Cox, A. R. J.; McGowan, S. J.; Bycroft, B. W.; Salmond, G. P. C. *Trends Biotechnol.* **1997**, *15*, 458–464. (c) Winans, S. C. *Trends Microbiol.* **1998**, *6*, 382–383. (d) Parsek, M. R.; Greenberg, E. P. *Trends Microbiol.* **2005**, *13*, 27–33. (e) Dong, Y. H.; Zhang, L. H. *J. Microbiol.* **2005**, *43*, 101–109.

(2) (a) Fuqua, C.; Parsek, M. R.; Greenberg, E. P. *Annu. Rev. Genet* **2001**, *35*, 439–468. (b) Whitehead, N. A.; Barnard, A. M. L.; Slater, H.; Simpson, N. J. L.; Salmond, G. P. C. *FEMS Microbiol. Rev.* **2001**, *25*, 365–404. (c) Miller, M. B.; Bassler, B. L. *Annu. Rev. Microbiol.* **2001**, *55*, 165–199. (d) Schaefer, A. L.; Greenberg, E. P.; Oliver, C. M.; Oda, Y.; Huang, J. J.; Bittan-Banin, G.; Peres, C. M.; Schmidt, S.; Juhaszova, K.; Sufrin, J. R.; Harwood, C. S. *Nature* **2008**, *454*, 595–600.

(3) (a) Welch, M.; Todd, D. E.; Whitehead, N. A.; McGowan, S. J.; Bycroft, B. W.; Salmond, G. P. C. *EMBO J.* **2000**, *19*, 631–641. (b) Zhang, L. H.; Murphy, P. J.; Kerr, A.; Tate, M. E. *Nature* **1993**, *362*, 446–448.

(4) (a) Fray, R. G.; Throup, J. P.; Daykin, M.; Wallace, A.; Williams, P.; Stewart, G. S. A. B.; Grierson, D. *Nat. Biotechnol.* **1999**, *17*, 1017–1020. (b) Dong, Y. H.; Gusti, A. R.; Zhang, Q.; Xu, J. L.; Zhang, L. H. *Appl. Environ. Microbiol.* **2002**, *68*, 1754–1759. (c) Lee, S. J.; Park, S. Y.; Lee, J. J.; Yum, D. Y.; Koo, B. T.; Lee, J. K. *Appl. Environ. Microbiol.* **2002**, *68*, 3919–3924. (d) Dong, Y. H.; Xu, J. L.; Li, X. Z.; Zhang, L. H. *Proc. Natl. Acad. Sci. U.S.A.* **2000**, *97*, 3526–3531.
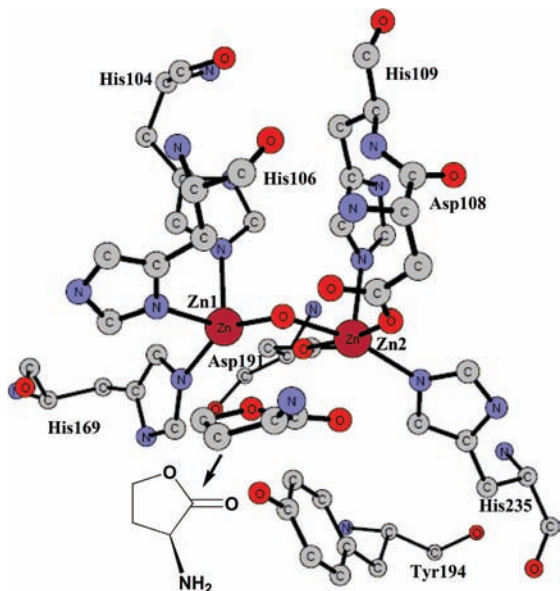
Figure 1. X-ray structure of the dinuclear zinc active site in AHL lactonase from *Bacillus thuringiensis* in complex with the inhibitor L-homoserine lactone (coordinates taken from PDB 2BR6[8b]).

indispensable for enzymatic activity.[7] Amino acid sequence alignments reveal a conserved HXHXDH motif, similar to the metallo-β-lactamase superfamily of enzymes.[4d] The X-ray crystal structure of AHL lactonase has been solved at high-resolution.[8] It shows an active site containing a dinuclear zinc center bridged by an aspartate (Asp191) and an oxygen species, presumably a hydroxide (see Figure 1). In addition, the first-shell coordination sphere of the dizinc center includes five histidines (His104, His106, His109, His169, and His235) and an aspartate (Asp108). In the structure of AHL lactonase in complex with L-homoserine lactone (HSL), a second shell residue, Tyr194, forms a hydrogen bond with the inhibitor ester oxygen.[8b] The structure of AHL lactonase from *Agrobacterium tumefaciens* reveals an almost identical active site arrangement, with the exception of the substitution of Asn114 for Phe107 in AHL lactonase from *Bacillus thuringiensis*.[9]

On the basis of crystallographic, mutational, and kinetic studies and of data concerning related enzymes of the metallo-β-lactamase superfamily, the following reaction mechanism has been proposed for AHL lactonase.[8] After substrate docking, the bridging hydroxide performs a nucleophilic attack at the carbonyl carbon to form a tetrahedral intermediate that is stabilized by one of the zinc ions. This is then followed by a C–O bond cleavage step. Tyr194 could then act as a general acid protonating the leaving group. In the above-mentioned structure of AHL lactonase in complex with HSL, the inhibitor carbonyl oxygen interacts with Zn2 while the ring oxygen is sandwiched between Zn1 and the Tyr194 residue (see Figure 1).[8b] Assuming that the substrate binds in the same fashion as the HSL inhibitor, this implies that the Zn2 ion is responsible for the electrostatic stabilization of the tetrahedral intermediate, while Zn1 is responsible for the stabilization of the leaving group.[8b]

However, it is possible that the substrate binding mode shown in Figure 1 represents a nonproductive complex.[8a] It has been argued that the full substrate, with its long acyl chain, would fit poorly and clash with the walls of the binding pocket.[8a] Another binding mode was proposed in which the carbonyl oxygen instead coordinates to Zn1 and the ring oxygen to Zn2.[8a] The roles of the zinc ions would then be reversed.

Very recently, support to this substrate binding mode was obtained from high-resolution crystal structures of the enzyme with products bound.[10a] Furthermore, quantum mechanics/molecular mechanics (QM/MM) molecular dynamics simulations show a stable ES complex only for this mode, with the less hindered *re* face of the lactone facing the dinuclear zinc site.[10b] In these studies, it was also proposed that it is the Asp108 residue (and not Tyr194) that shuttles the proton during the reaction, since in the enzyme–product structures it was found to lose its coordination to Zn2 and form a hydrogen bond to the hydroxyl leaving group of the product.

In the current work, the density functional theory method B3LYP[11] was employed to investigate the reaction mechanism of AHL lactonase. A model of the active site was designed on the basis of the crystal structure, and the potential energy surfaces for the reactions of both substrate orientations were calculated. This approach has previously been successfully applied to study a number of enzyme reaction mechanisms,[12] including four recent studies on the reaction mechanisms of the related dinuclear zinc enzymes phosphotriesterase (PTE),[13a] aminopeptidase from *Aeromonas proteolytica* (AAP),[13b] dihydroorotase (DHO),[13c] and Glyoxalase II (GlxII).[13d] A detailed understanding of the reaction mechanism of the AHL lactonase enzyme family will be helpful for developing more effective quorum-quenching agents.

(5) (a) Lin, Y. H.; Xu, J. L.; Hu, J. Y.; Wang, L. H.; Ong, S. L.; Leadbetter, J. R.; Zhang, L. H. *Mol. Microbiol.* **2003**, *47*, 849–860. (b) Huang, J. J.; Han, J. I.; Zhang, L. H.; Leadbetter, J. R. *Appl. Environ. Microbiol.* **2003**, *69*, 5941–5949. (c) Park, S. Y.; Kang, H. O.; Jang, H. S.; Lee, J. K.; Koo, B. T.; Yum, D. Y. *Appl. Environ. Microbiol.* **2005**, *71*, 2632–2641. (d) Romero, M.; Diggle, S. P.; Heeb, S.; Cámara, M.; Otero, A. *FEMS Microbiol. Lett.* **2008**, *280*, 73–80.

(6) (a) Suga, H.; Smith, K. M. *Curr. Opin. Chem. Biol.* **2003**, *7*, 586–591. (b) Alksne, L. E.; Projan, S. J. *Curr. Opin. Biotechnol.* **2000**, *11*, 625–636. (c) Dong, Y. H.; Wang, L. H.; Xu, J. L.; Zhang, H. B.; Zhang, X. F.; Zhang, L. H. *Nature* **2001**, *411*, 813–817.

(7) Thomas, P. W.; Stone, E. M.; Costello, A. L.; Tierney, D. L.; Fast, W. *Biochemistry* **2005**, *44*, 7559–7569.

(8) (a) Liu, D. L.; Lepore, B. W.; Petsko, G. A.; Thomas, P. W.; Stone, E. M.; Fast, W.; Ringe, D. *Proc. Natl. Acad. Sci. U.S.A.* **2005**, *102*, 11882–11887. (b) Kim, M. H.; Choi, W.-C.; Kang, H. O.; Lee, J. S.; Kang, B. S.; Kim, K. J.; Derewenda, Z. S.; Oh, T.-K.; Lee, C. H.; Lee, J.-K. *Proc. Natl. Acad. Sci. U.S.A.* **2005**, *102*, 17606–17611.

(9) Liu, D. L.; Thomas, P. W.; Momb, J.; Hoang, Q. Q.; Petsko, G. A.; Ringe, D.; Fast, W. *Biochemistry* **2007**, *46*, 11789–11799.

(10) (a) Liu, D.; Momb, J.; Moulin, A.; Petsko, G. A.; Fast, W.; Ringe, D. *Biochemistry* **2008**, *47*, 7706–7714. (b) Momb, J.; Wang, C.; Liu, D.; Thomas, P. W.; Petsko, G. A.; Guo, H.; Ringe, D.; Fast, W. *Biochemistry* **2008**, *47*, 7715–7725.

(11) (a) Becke, A. D. *J. Chem. Phys.* **1993**, *98*, 5648–5652. (b) Lee, C.; Yang, W.; Parr, R. G. *Phys. Rev. B: Condens. Matter Mater. Phys.* **1988**, *37*, 785–789.

(12) See for example the following reviews: (a) Himo, F.; Siegbahn, P. E. M. *Chem. Rev.* **2003**, *103*, 2421–2456. (b) Noodleman, L.; Lovell, T.; Han, W.-G.; Li, J.; Himo, F. *Chem. Rev.* **2004**, *104*, 459–508. (c) Siegbahn, P. E. M.; Borowski, T. *Acc. Chem. Res.* **2006**, *39*, 729–738. (d) Himo, F. *Theor. Chem. Acc.* **2006**, *116*, 232–240. (e) Ramos, M. J.; Fernandes, P. A. *Acc. Chem. Res.* **2008**, *41*, 689–698.
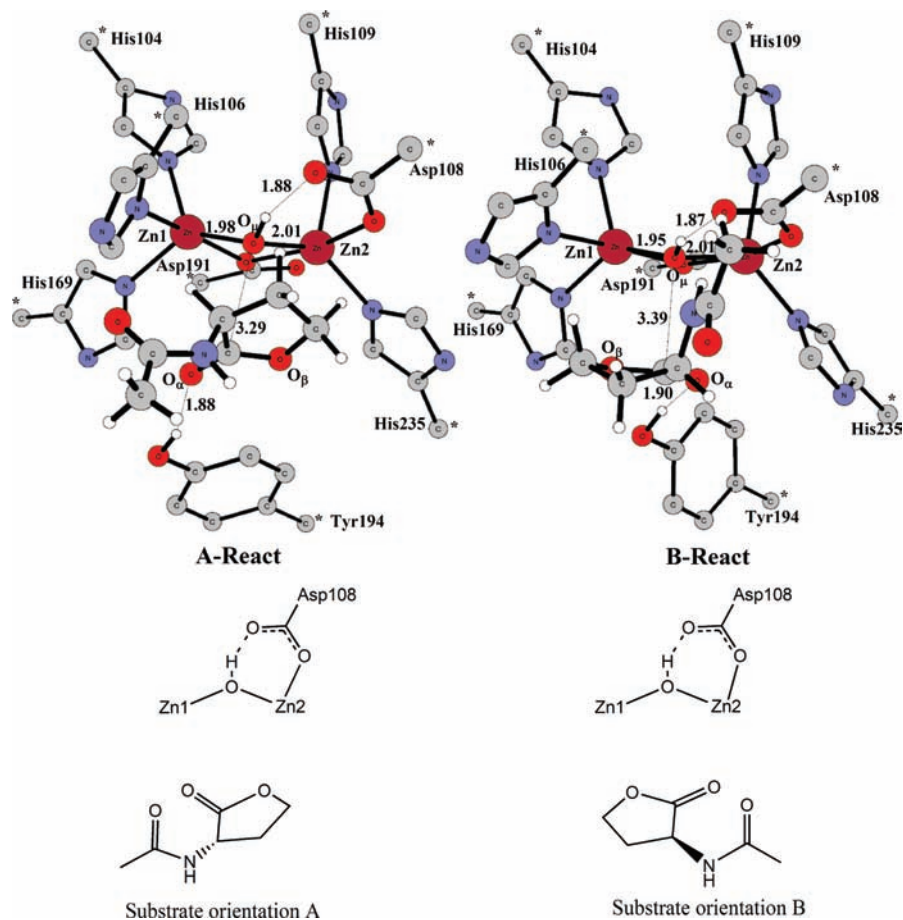
Figure 2. Optimized structures for the active site model of AHL lactonase. Two different substrate orientations are considered. For clarity, some hydrogen atoms are omitted in the figures. Atoms marked with asterisks were fixed at their X-ray positions during the geometry optimizations. Distances are given in angstroms (Å).

II. Computational Details

All calculations were carried out using the B3LYP hybrid density functional theory method.[11] For the geometry optimization, the 6-31G(d,p) basis set was used for the C, N, O, and H elements and the LANL2DZ pseudopotential for zinc ions. On the basis of these geometries, more accurate energies were obtained by performing single-point calculations using the 6-311+G(2d,2p) basis set for all elements. Frequency calculations were performed at the same level of theory as the geometry optimizations on all of the stationary points of the reaction path, to establish their character and to evaluate the zero-point vibrational energy corrections. The solvation corrections were calculated at the same theory level as the geometry optimizations from single-point calculations on the optimized structures using the CPCM method.[14] A dielectric constant of 4 was used to model the parts of the enzyme that are not included in the quantum chemical active site model. A number of atoms, where truncations were made, were kept fixed to their crystallographically observed positions to preserve the overall structure of the active

site. This procedure leads to a few small imaginary frequencies typically on the order of $10i-40i$ cm^{-1}. These do not affect the obtained energetic results significantly, but render the evaluation of the harmonic entropy effects unreliable. Therefore, entropy was not considered in the present study. Finally, all computations were carried out with the Gaussian 03 code.[15]

III. Model of Active Site

A model of the AHL lactonase active site was constructed on the basis of the crystal structure solved for the enzyme complexed with L-homoserine lactone (PDB code 2BR6).[8b] The first-shell coordination sphere was modeled by five methyl-imidazoles that simulate the His104, His106, His109, His169, and His235 residues and two acetates that mimic the Asp108 and Asp191 residues. A hydroxide was used as the bridging nucleophile oxygen species. Tyr194, an important second-shell residue, was also included, modeled by p-methyl-phenol. Hydrogen atoms were added manually, and bonds that were truncated were saturated by hydrogen atoms. To keep the optimized structures close to the experimental ones, the truncation atoms were kept fixed to their X-ray positions during the geometry optimizations. The fixed atoms are marked with an asterisk in the figures below. As a model substrate, we chose N-acetyl homoserine lactone (see Figure 2), which is adequate to study the chemical steps of the AHL

(13) (a) Chen, S.-L.; fang, W.-H.; Himo, F. *J. Phys. Chem. B* **2007**, *111*, 1253–1255. (b) Chen, S.-L.; Marino, T.; Fang, W.-H.; Russo, N.; Himo, F. *J. Phys. Chem. B* **2008**, *112*, 2494–2500. (c) Liao, R.-Z.; Yu, J.-G.; Raushel, F. M.; Himo, F. *Chem.—Eur. J.* **2008**, *14*, 4287–4292. (d) Chen, S.-L.; Fang, W.-H.; Himo, F. *J. Inorg. Biochem.* **2008**,in press.
(14) (a) Barone, V.; Cossi, M. *J. Phys. Chem. A* **1998**, *102*, 1995–2001. (b) Cammi, R.; Mennucci, B.; Tomasi, J. *J. Phys. Chem. A* **1999**, *103*, 9100–9108. (c) Klamt, A.; Schüürmann, G. *J. Chem. Soc., Perkin. Trans.* **1993**, *2*, 799–805. (d) Tomasi, J.; Mennucci, B.; Cammi, R. *Chem. Rev.* **2005**, *105*, 2999–3094.
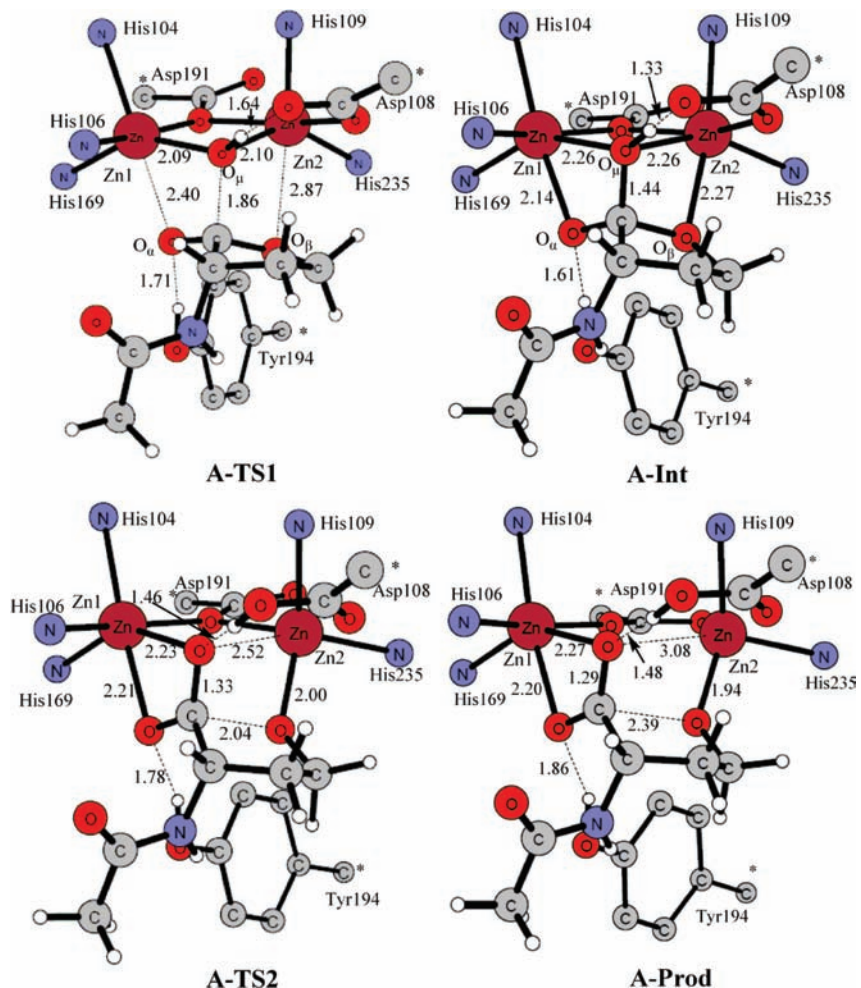
Figure 3. Optimized geometries of the transition states and intermediates along the reaction pathway for substrate orientation A. For clarity, the imidazole ligands are represented by only a nitrogen atom in the figures.

lactonase reaction. The total size of the model is thus 113 atoms, and the total charge is +1.

IV. Results and Discussions

As briefly discussed above, two different substrate orientations have been suggested (called A and B here).[8] In orientation A, the substrate binds with its carbonyl oxygen coordinated to Zn1 and the leaving oxygen coordinated to Zn2, while in the alternative orientation B, the coordination is reversed. In this study, we consider both of these options.

The optimized structures of the active site model in complex with the model substrate, corresponding to the Michaelis complex in the two different orientations (here called reactants, **A-React** and **B-React**), are displayed in Figure 2. We first note that none of the substrate oxygens coordinates to any of the zinc ions in the Michaelis complexes of any of the two substrate orientations. The distances between zinc ions and carbonyl oxygen (O_α) or the ring oxygen (O_β) are around 4 Å. The fact that the substrate carbonyl does not coordinate to the metal ions in the Michaelis complex appears to be a quite common theme, as similar observations were made for other hydrolytic dinuclear zinc enzymes, such as AAP,[13b] DHO,[13c] and GlxII.[13d]

In **B-React**, we note that the substrate amide forms a weak hydrogen bond to Asp108, an interaction that is not present

in **A-React** (see Figure 2). Since the substrate does not coordinate to the zinc ions in the Michaelis complexes, the calculated energies for the two substrate orientations are very similar using this current active site model. Orientation A is favored by only 0.5 kcal/mol over orientation B. The Zn–Zn distance is calculated to be 3.21 and 3.24 Å for orientations A and B, respectively, in good agreement with the crystal structure result (3.33 Å).

A. Hydrolysis through Substrate Orientation A. Starting from **A-React**, we have optimized the structures of the transition state for the nucleophilic attack (**A-TS1**) and the resulting tetrahedral intermediate (**A-Int**) for orientation A (shown in Figure 3). The barrier is calculated to be 16.4 kcal/mol, and **A-Int** is found to lie 14.1 kcal/mol higher than **A-React**. We find that the nucleophilic attack occurs directly from the bridging position, similarly to the other dinuclear zinc enzymes that we have studied previously, namely, PTE,[13a] AAP,[13b] DHO,[13c] and GlxII.[13d] **A-TS1** is characterized by an imaginary frequency of 197i cm^{-1}. The critical O_μ–C distance is 1.86 Å, and the ester C–O_β and carbonyl C–O_α bonds are elongated to 1.38 and 1.26 Å, respectively. At **A-Int**, these two bonds are elongated further to 1.49 and 1.32 Å, respectively, while the O_μ–C becomes 1.44 Å. The bond distance between the carbonyl oxygen and Zn1 is
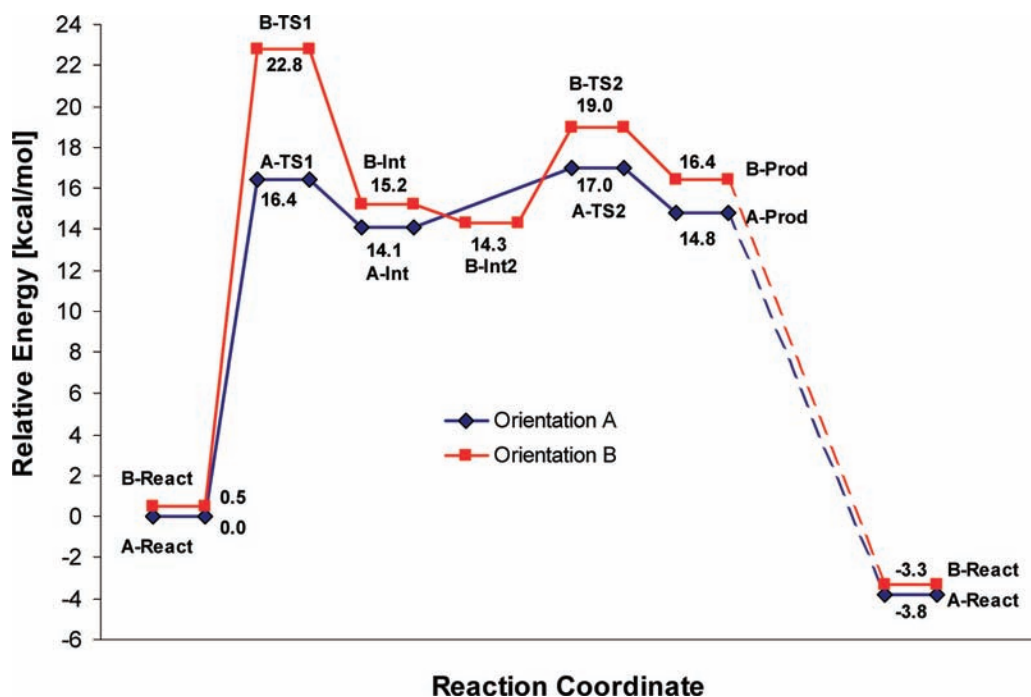
Figure 4. Calculated potential energy profiles for N-acyl-L-homoserine lactone hydrolysis in the two different substrate orientations.

shortened considerably, from essentially no interaction in **A-React** to 2.40 Å at **A-TS1** and 2.14 Å at **A-Int**. This shows that the Zn1 ion provides electrostatic stabilization to the transition state and the tetrahedral intermediate, thereby lowering the barrier for the nucleophilic attack. In addition, the hydrogen bond from Tyr194 to O_α becomes stronger, as indicated by the decrease of the hydrogen bond distance from 1.88 Å in **A-React** to 1.71 Å at **A-TS1** and 1.61 Å at **A-Int** (see Figures 2 and 3). This shows that the Tyr194 residue provides further stabilization to the TS and the tetrahedral intermediate, in line with previous suggestions based on the crystal structure.[8a] The O_μ is still bridging the two zinc centers with two equal distances of 2.26 Å at **A-Int**. The shortening of the hydrogen bond between Asp108 and the bridging hydroxide from 1.88 Å in **A-React** to 1.33 Å in **A-Int** implies that also this residue plays a role in stabilizing the tetrahedral intermediate. We furthermore notice that during the nucleophilic attack the interaction between Zn2 and the oxygen of the five-membered ring (O_β) becomes stronger (Zn2$-O_\beta$ distance is 2.27 Å at **A-Int**). This interaction will be important for the dissociation of the C$-O_\beta$ bond in the next step.

The second part of the reaction is the C$-O_\beta$ bond cleavage, resulting in the opening of the five-membered ring. The transition state for this (called **A-TS2**) was optimized and is also shown in Figure 3. It was found that, simultaneously with the C$-O_\beta$ bond cleavage, a proton is transferred from the bridging oxygen to Asp108. The critical C$-O_\beta$ distance is 2.04 Å, and the transition state is characterized by an imaginary frequency of $109i$ cm^{-1}. The calculated energy of **A-TS2** is 2.9 kcal/mol higher than that of **A-Int** (i.e., 17.0 kcal/mol higher than that of **A-React**). The resulting structure corresponds to the dinuclear zinc cluster in complex with the deprotonated product (**A-Prod**, Figure 3). The energy of this complex is calculated to be 14.8 kcal/mol higher than that of **A-React**. In

A-Prod, the newly formed carboxylate coordinates to Zn1 in a bidentate fashion. Due to the negative charge at the alkoxide O_β, the Zn2$-O_\beta$ bond distance decreases from 2.27 Å in **A-Int** to 1.94 Å in **A-Prod** (2.00 Å in **A-TS2**). The Zn2 ion thus plays an important role in stabilizing the emerging alkoxide, facilitating thereby the ring opening step.

To complete the reaction, the product has to be released from the active site and a water molecule has to enter and regenerate the bridging hydroxide ligand. The product can either be released in the anionic form or possibly receive a proton from the Tyr194[8b] or the Asp108 residues. One way to estimate the overall energetics involved in this process is to calculate the overall driving force involved in the AHL lactonase reaction. We have calculated that the hydrolysis reaction of Scheme 1 is exothermic by 3.8 kcal/mol. Since the enzyme does not alter this energy, one full enzyme cycle should also be exothermic by the same amount. Thus, one can estimate that the steps involved in the product release, active site regeneration, and the binding of a new substrate to the active site are in total exothermic by ca. 18.6 kcal/mol (which is the energy of **A-Prod** added to the overall exothermicity, i.e., 14.8 + 3.8 kcal/mol).

The calculated energy profile for the reaction mechanism is displayed in Figure 4. The overall barrier of 17 kcal/mol is in very good agreement with the experimental k_{cat}, which was found to lie in the range of 20−650 s^{-1} for AHLs with different lengths of the acyl chain.[7,10b,15,16] Using classical transition state theory, these rate constants can be converted to barriers of 14−16 kcal/mol.

As seen from Figure 4, the calculated energy difference between **A-TS1** and **A-TS2** is too small (0.5 kcal/mol) to be able to unambiguously distinguish which one of them is the rate-limiting step. However, the fact that the transition state for ring opening is slightly higher is consistent with the experimentally observed thio effect.[16] Hydrolysis of
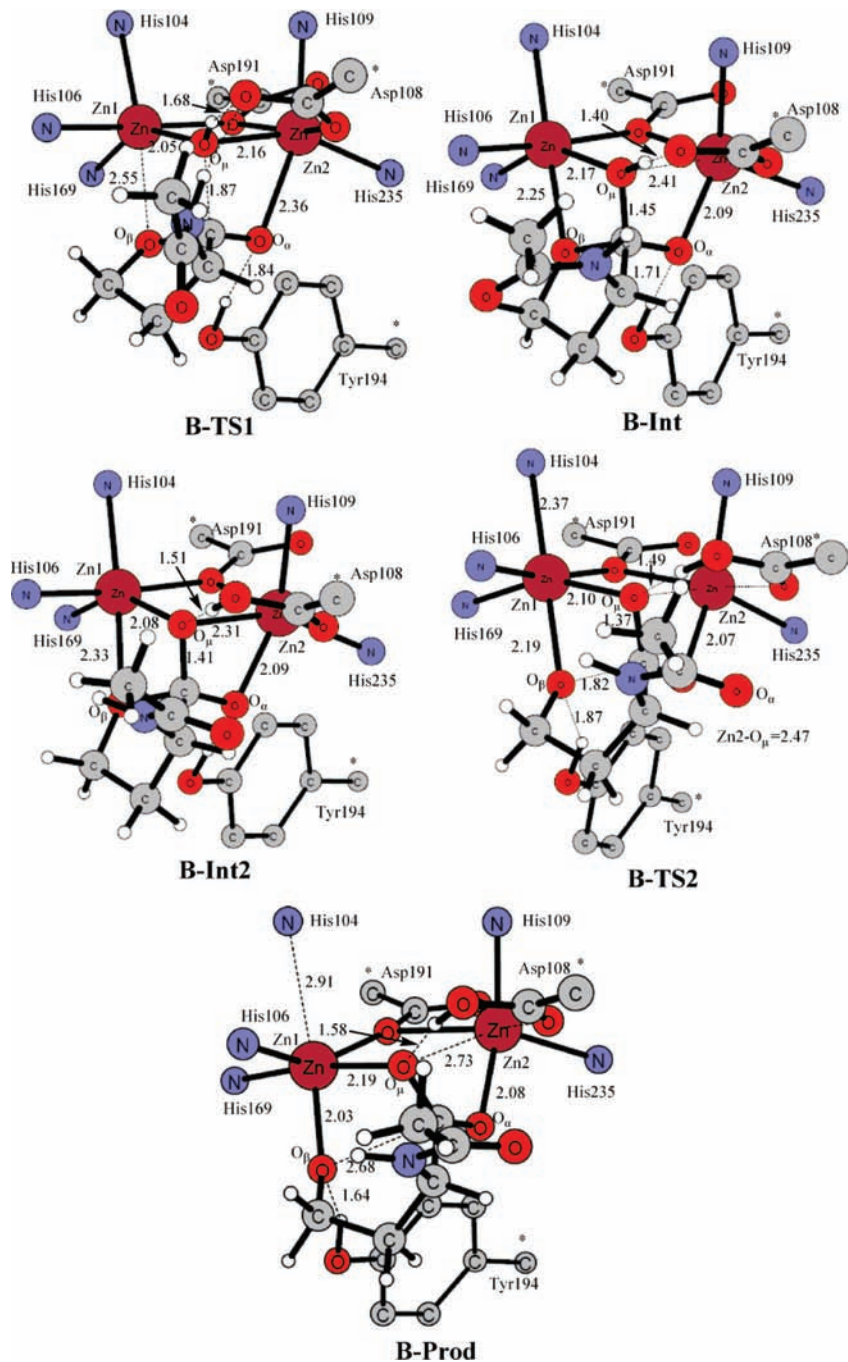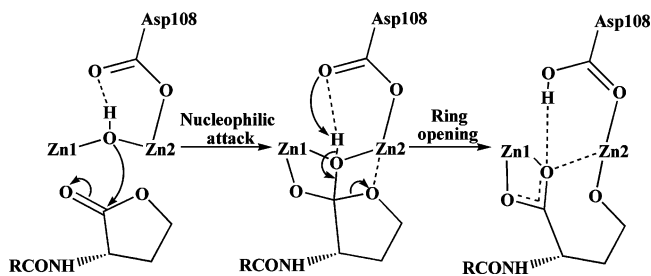
Figure 5. Optimized geometries of transition states and intermediates along the reaction pathway for substrate orientation B.

Scheme 2. Reaction Mechanism of AHL Lactonase

N-hexanoyl-L-homoserine lactone and its corresponding thiolactone by AHL lactonase disubstituted with Mn^{2+}, Co^{2+}, Zn^{2+}, and Cd^{2+} indicated a kinetically significant interaction between the metal and the leaving group.[16]

B. Hydrolysis through Substrate Orientation B. The calculated energetics of substrate orientation A described above agree quite well with the available experimental kinetic information, such as the k_{cat} and the thio effect. It is also in line with the very recent results obtained from the enzyme–product crystal structures[10a] and from the QM/MM simulations.[10b] The enzyme–inhibitor structure, however, suggests that the substrate docks to the active site according to orientation B (see Figure 2).[8b] We therefore optimized the stationary points of the hydrolysis reaction for this orientation, in a similar fashion as for orientation A above.

The optimized transition state for nucleophilic attack (**B-TS1**) and the resulting tetrahedral intermediate (**B-Int**) are

displayed in Figure 5. The local structure of the transition state is quite similar to that of **A-TS1**. The nucleophilic attack occurs from a bridging position, and the $C-O_\mu$ distance at the transition state is 1.87 Å (1.86 Å in **A-TS1**). However, the barrier is calculated to be 22.3 kcal/mol, which is 5.9 kcal/mol higher than the corresponding barrier in binding mode A. The resulting tetrahedral intermediate **B-Int** lies at +14.7 kcal/mol relative to **B-React**. It is interesting to note that, in **B-Int**, the bridging O_μ becomes slightly asymmetric, with distances of 2.17 and 2.41 Å to Zn1 and Zn2, respectively. We can see two reasons for the higher barrier observed in this substrate orientation. The main reason is that, since the binding is reversed, Zn2 is now providing electrostatic stabilization to the transition state and the tetrahedral intermediate. However, because of the different ligand fields, Zn1 and Zn2 are not symmetric. In particular, the negatively charged Asp108 ligand makes Zn2 slightly less positively charged than Zn1, reducing thereby its catalytic effect. This is confirmed by the calculated Mulliken charges, which are +1.00e, +1.02e, and +0.99e for Zn1 in **A-React**, **A-TS1**, and **A-Int**, respectively, and +0.97e, +0.95e, and +0.92e for Zn2 in **B-React**, **B-TS1**, and **B-Int**, respectively. Another reason is the hydrogen bond between Tyr194 and the carbonyl oxygen. In orientation A, the H···O distance is 1.88, 1.71, and 1.61 Å in **A-React**, **A-TS1**, and **A-Int**, respectively (see Figures 2 and 3), while in orientation B, the corresponding distances are 1.90, 1.84, and 1.71 Å, respectively (see Figures 2 and 5).

For the following ring opening step, we found that the proton transfer from μ-OH to Asp108 occurs as a separate step. We located a distinct intermediate (**B-Int2**, Figure 5), in which the proton resides on Asp108 and the hydrogen bond from the amide of the substrate to Asp108 is broken. **B-Int2** lies only 0.9 kcal/mol lower than **B-Int**. The transition state for the ring opening was located, with a $C-O_\beta$ distance of 1.82 Å (**B-TS2**, Figure 5). The barrier is calculated to be 4.7 kcal/mol higher than **B-Int2** (Figure 4). The resulting enzyme−product complex, **B-Prod**, is 15.9 kcal/mol higher than **B-React**. In **B-prod**, the newly formed carboxylate

binds to both zinc ions, in contrast to **A-Prod**, where the carboxylate binds bidentately to Zn1.

For orientation B, the nucleophilic attack is clearly the rate-limiting step (see Figure 4). The high barrier, however, shows that this substrate orientation is not productive, which explains why the HSL inhibitor itself is not hydrolyzed.

V. Conclusions

In this paper, we have investigated the reaction mechanism of N-acyl-L-homoserine lactone hydrolysis by AHL lactonase. Following previous proposals,[8] two possible mechanisms based on two different substrate orientations were considered (see Figure 2). The optimized geometries of the stationary points are displayed in Figures 2, 3, and 5, and the calculated potential energy profiles are shown in Figure 4.

Our calculations show that the reaction mechanism shown in Scheme 2 (corresponding to substrate orientation A) is energetically more feasible and is in agreement with available experimental kinetic and structural data. In this mechanism, the substrate binds to the active site without direct coordination to any of the zinc ions. The bridging hydroxide then acts as a nucleophile, attacking the carbonyl carbon of the substrate. The Zn1 ion, along with Tyr194, stabilizes the oxyanion of the tetrahedral intermediate, thereby lowering the barrier for the nucleophilic attack. Zn2, on the other hand, facilitates the ring opening step by stabilizing the leaving group.

From the calculations, it is difficult to determine which one, the nucleophilic attack or the ring opening step, is the rate-limiting step, since the barriers are too close (16.4 and 17.0 kcal/mol, respectively). However, the fact the latter is slightly higher is consistent with the experimentally observed thio effect.[16]

The alternative substrate orientation B, which corresponds to the X-ray structure solved for the enzyme in complex with the L-homoserine lactone inhibitor (see Figures 1 and 2), is shown to be a nonproductive binding mode. The barrier for the nucleophilic attack is sufficiently higher than that for orientation A (22.8 vs 16.4 kcal/mol) and can be discarded. The reasons are the poorer electrostatic stabilization of the tetrahedral intermediate provided by the Zn2 ion compared to Zn1 and also the weaker stabilization provided by the hydrogen bond to the Tyr194 residue.

Finally, the present study shows that, although the quantum chemical models used here are too small to conduct docking-like studies to be able to distinguish between different binding modes, accurate energies of the following chemical steps obtained with DFT methods are able to do so.

(15) (a) Frisch, M. J.; Trucks, G. W.; Schlegel, H. B.; Scuseria, G. M. E.; Robb, A.; Cheeseman, J. R.; Montgomery, J. A., Jr.; Vreven, T.; Kudin, K. N.; Burant, J. C.; Millam, J. M.; Iyengar, S. S.; Tomasi, J.; Barone, V.; Mennucci, B.; Cossi, M.; Scalmani, G.; Rega, N.; Petersson, G. A.; Nakatsuji, H.; Hada, M.; Ehara, M.; Toyota, K.; Fukuda, R.; Hasegawa, J.; Ishida, M.; Nakajima, T.; Honda, Y.; Kitao, O.; Nakai, H.; Klene, M.; Li, X.; Knox, J. E.; Hratchian, H. P.; Cross, J. B.; Adamo, C.; Jaramillo, J.; Gomperts, R.; Stratmann, R. E.; Yazyev, O.; Austin, A. J.; Cammi, R.; Pomelyli, C.; Ochterski, J. W.; Ayala, P. Y.; Morokuma, K.; Voth, G. A.; Salvador, P.; Dannenberg, J. J.; Zakrzewski, V. G.; Dapprich, S.; Daniels, A. D.; Strain, M. C.; Farkas, O.; Malick, D. K.; Rabuck, A. D.; Raghavachari, K.; Foresman, J. B.; Ortiz, J. V.; Cui, Q.; Baboul, A. G.; Clifford, S.; Cioslowski, J.; Stefanov, B. B.; Liu, G.; Liashenko, A.; Piskorz, P.; Komaromi, I.; Martin, R. L.; Fox, D. J.; Keith, T.; Al-Laham, M. A.; Peng, C. Y.; Nanayakkara, A.; Challacombe, M.; Gill, P. M. W.; Johnson, B.; Chen, W.; Wong, M. W.; Gonzalez, C.; Pople, J. A. *Gaussian 03*, revision D.01; Gaussian, Inc.: Pittsburgh, PA, 2004. (b) Wang, L.-H.; Weng, L.-X.; Dong, Y.-H.; Zhang, L.-H. *J. Biol. Chem.* **2004**, *279*, 13645–13651.
(16) Momb, J.; Thomas, P. W.; Breece, R. M.; Tierney, D. L.; Fast, W. *Biochemistry* **2006**, *45*, 13385–13393.